

Optimization of Passenger and Freight Co-transportation Schemes based on Virtual Formation for Large and Small Interchanges in Airport Railway Lines

Zunzun Hou, Ruichun He, Shixiang Wan, Cunjie Dai

Abstract — The real-time dynamic coupling under the virtual-coupling technology guarantees running multi-group trains in different sections based on passenger flow's spatial and temporal distribution characteristics. It enables more flexible transport organization modes such as full-length and short-turn routing and the express/local stop mode. Utilizing the redundant capacity of the airport line to carry out coordinated transportation of passengers and goods is an essential means of relieving urban traffic pressure, saving energy, and protecting the environment. To promote urban rail transit to achieve the goal of "double-carbon," the optimization of passenger and freight cooperative transport schemes based on the virtual coupling technology for the airport line of the rail transit is investigated. Based on the train operation of full-length and short-turn routing under the virtual-coupling technology, according to the unbalanced distribution characteristics of passenger and freight flows in urban rail transit, this paper constructs an optimization model of urban rail transit capacity allocation to minimize passenger travel costs, enterprise operation costs, and carbon emission costs, and considering the constraints of the carbon emission policy, with the constraints such as the train operation safety, the constraints of the balance of the passenger flow and freight flow loading. The multi-objective model to solve the optimization problem has been designed. Given the complexity of the multi-objective model solution, an improved non-dominated sorting genetic algorithm is designed, and the algorithm makes use of the screening function of the constraints during the initial population generation process, which effectively balances the relationship between the whole process of screening and time-consumption of the NSGA-II algorithm. Taking Wuxi Metro Line 3 as an example, the results show that: (i) Compared with the traditionally large and small crossing mode, full-length and short-turn routing of virtual coupling Trains proposed in this paper can reduce the average waiting time of passengers by about 2.01min, the cost of carbon emission by 15.7% and the cost of enterprise operation by 20.2%, and at the same time, improve the average total rate by about 50%, which verifies that the virtual

formation technology is conducive to improving the efficiency of passenger travel and reducing the operating cost and the carbon cost. It is also beneficial for improving passenger traveling efficiency. (ii) The single-alignment fixed configuration mode, compared with the single-flow mode, can increase the average full-load rate by 26.6% while increasing the passenger travel cost by only 0.98% and reducing the carbon emission cost by a small margin; the virtual configuration technology based on the large and small-alignment operation and transport scheme increases the passenger travel cost by about 0.3% and further reduces the carbon emission cost by 1.9%. They further reduced the carbon emission cost by 1.9% while increasing the average total occupancy rate by about 5.8%. The proposed models and algorithms provide some decision support for urban rail transit operators to optimize transport schemes under different carbon emission policies and the virtual coupling operation mode.

Index Terms—Urban rail transit; Virtual coupling; Metro freight coordination transportation; Full-length Routes; NSGA-II

I. INTRODUCTION

Murakami [1] pointed out that there is a negative correlation between the productivity of the city where the airport is located and the travel time from the city center to the airport by rail. Using urban rail transit airport lines to carry out freight services can help build a green and intensive urban logistics system [2]. At the same time, it can also bring additional freight revenue for the operating companies. [3] pointed out that by making full use of the redundant capacity of the subway lines in the off-peak period, the development of subway-coordinated transportation of the underground logistics network has become a more feasible solution. [4] argued that developing there are more viable options than underground logistics networks based on event-based simulation models and the practice of the Newcastle metro section. Demonstrated the feasibility and advantages of underground logistics distribution based on the simulation model of events and the practice of the Newcastle metro section. [5] Moreover, [6] investigated the optimization of existing passenger train set piggyback mode and high-speed rail express train based on the determined demand, which provided a reference for the rail transport freight transport research. [7] used the SIMUL8 to build a baggage check-in system based on the Nexus subway system. SIMUL8 constructed a baggage checking system based on the Nexus subway system, running freight trains between 2 airports to transport

Manuscript received February 15, 2024; revised June 24, 2024.

This work was supported in part by Young-Doctor Found Project of Gansu Province Higher Education (No. 2022QB-065) and Natural Science Foundation of Gansu Province(23JRRA858).

Zunzun Hou is a postgraduate student at School of Traffic and Transportation, Lanzhou Jiaotong University, Lanzhou 730070, China. (e-mail: yvni99@126.com).

Ruichun He is a Professor at School of Traffic and Transportation, Lanzhou Jiaotong University, Lanzhou 730070, China. (e-mail: Herc@mail.lzjtu.cn).

Shixiang Wan is a postgraduate student at School of Traffic and Transportation, Lanzhou Jiaotong University, Lanzhou 730070, China. (e-mail: 13541950798@163.com).

Cunjie Dai is a Professor at School of Traffic and Transportation, Lanzhou Jiaotong University, Lanzhou 730070, China. (e-mail: daicunjie@mail.lzjtu.cn).

baggage. [8] studied the train schedule optimization of additional freight trains, [9] studied the use of the remaining space of the passenger cars of the train schedule optimization problem. [10] based on the passenger and freight co-traffic and freight trains in 2 forms, studied the train stopping scheme and the train stopping scheme based on the passenger and freight co-traffic. The train stopping scheme and train schedule were studied. [11] Analyze the train schedules of metro passengers and freight cars to minimize the weighted sum of the operating costs and the total delay penalties. The objective is to analyze the co-optimization problem of metro passenger and freight car arrangement and flow management. [12] considered the optimization of train formation and co-optimization of passenger and freight transport under flexible formation conditions to obtain the operation diagram, train formation scheme, and co-optimization of passenger and freight transport scheme for system optimization.[13] studied the problem of inserting freight trains under the premise of fixed passenger trains to optimize the timetable and stopping scheme of freight trains. [14] constructed an urban rail transit passenger and freight mixing optimization model to optimize the energy consumption of urban rail transit carriages to minimize the waiting time of passengers and freight and the energy consumption of train carriages.[15] evaluated the carbon emissions of the operational phase of the urban rail system, and the study showed that the carbon emissions generated during the operational phase accounted for 82% of the system, and the train carbon emissions and the station carbon emissions accounted for 50% and 42%, respectively.[16] used the VB program to establish a calculation model of carbon emissions from vehicles and stations in the operation phase of urban rail transit. [17] constructed the optimization scheme of large and small interchanges to reduce passenger travel costs, carbon emissions generated by trains, and corporate operating costs.[18] constructed an optimization model of urban rail transit passenger and freight mixing to optimize the energy consumption of urban rail transit carriages to minimize the waiting time of passengers and goods and the energy consumption of the train carriages.

Most large and small traffic routing schemes aim to minimize passenger waiting costs and enterprise operating costs. [19][20][21][22] establish the optimization model of the running scheme from the perspective of both passengers and enterprises to minimize the total cost of both. The safety of virtual formation technology is an important research direction. [23] put forward the concept of virtual formation train operation safety and proposed a safety analysis method based on a conditional event network,[24] modeled and verified the typical scenarios under the virtual formation mode of trains, and the results showed that the virtual formation trains are as safe as the traditional trains. [25][26][27] established the model of the passing capacity of virtual formation trains to Examples demonstrate that this technique can improve the line throughput capacity.[28] proposed a real-time de-knitting operation organization method for fast and slow trains using virtual knitting technology, and [29] proposed an algorithm for generating a virtual knitting train operation scheme in which each car operates according to a fixed periodic stopping scheme

without considering the influence of the difference in passenger flow at different stations, which is not practical. [30][31] propose an optimization model for virtual formation trains to optimize the number of trains on a unidirectional loop line based on which a more complex Y-shaped line is used to optimize the train routes to satisfy the passengers' travel demand.

The main contributions of this study are as follows: (i) This paper investigates a new class of urban rail passenger/cargo co-operation optimization problem based on the original passenger outgoing cost and enterprise operating cost, which is dominated by low-carbon objectives and can be adapted to the differences in carbon emission policies, considering the interests of passengers, enterprises and the environment. (ii) In this paper, under the traditionally large and small crossing operation mode of urban rail transit, the problem of urban rail passenger and freight cooperative transport under virtual grouping technology is studied. A new type of scenario is put forward: trains are grouped and ungrouped at the small crossing return point, which can better realize the balance of the total load rate of the whole network and the interval between departures under the premise of satisfying the demand for matching the capacity of different crossing segments. (iii) based on a single passenger transport operation model, this paper investigates the use of redundant capacity in the peak period of the rail transit airport line to carry out coordinated transport of passengers and freight, to reduce the wastage of capacity, and to enhance the enterprise's profitability.

II. PROBLEM DESCRIPTION

In this paper, a composite urban rail transit airport line is taken as the object of study, noting that urban rail transit lines $L = \{S, E\}$, S and E denote the station set and interval set of the line, respectively, where $S = \{1, 2, \dots, S_a, \dots, i, \dots, j, \dots, S_b, \dots, S^{(n)}\}$, the line has a total of $S^{(n)}$ stations, and the times of $d = \{d|1, 2\}$, $d=1$ denote the upward direction, and the time of $d=2$ denotes the downward direction. The study period is divided into several equal-length operating periods, defined $T = \{1, 2, \dots, t, \dots, T^{(n)}\}$ as the set of operating periods, $T^{(n)}$ as the total number of periods, and σ as the length of the unit operating period.

A. Virtual Grouping Train Size Crossover Operation Mode

Consider an urban rail transit line. Fig.1 is a schematic diagram of the train size of the intersection operation scheme, in which the large intersection m_1 trains run through the whole line. The train runs from station 1 to station $S^{(n)}$ and then folds back.

The miniature intersection m_2 trains run for part of the section operation, the train runs from station S_a to station S_b and then folds back. Notation M_1 denotes the section where trains of large and small interchanges operate together, and the remaining section is denoted as M_{21}, M_{22} .

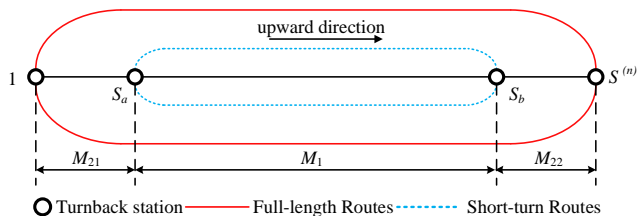


Fig. 1. Schematic Diagram of Train Plan with Full-length and Short-turn Routes

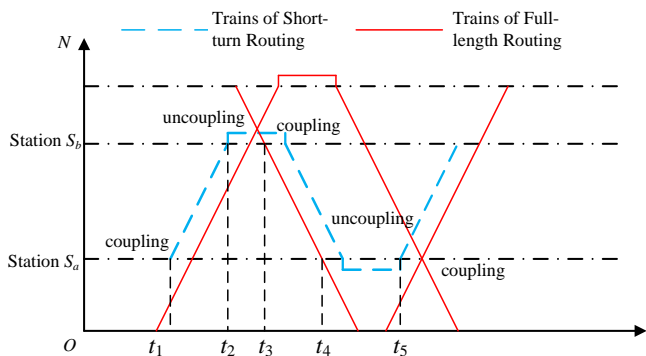


Fig. 2. Coupling Process with Full-length and Short-turn Routing of Virtual Coupling Trains

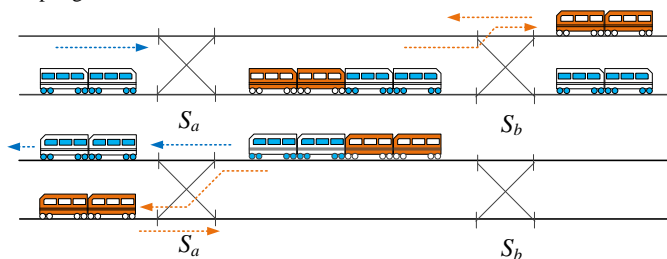


Fig. 3. Running Process with of Full-length and Short-turn Routing of Virtual Coupling Trains

Under virtual grouping technology, the transportation organization mode of large and small interchanges can be more flexible, and the train running path can have a new design. As shown in Figure 1, the small junction return station for S_a, S_b , is also the main line of a virtual grouping of the joint and ungrouping location, the two trains in the small junction section of the virtual reconnection operation, defined as *virtual reconnection of the train* for the larger passenger flow of the small junction section to provide a larger capacity, in the small junction when arriving at another small junction return station to be ungrouped, the large junction train continues to run forward, the small junction train in the folding station for folding operations, the formation of the large and small junction. The large-crossing train continues to run forward, and the small-crossing train carries out the folding operation at the folding station, forming a large and small crossroads. Fig.2 is a schematic diagram of the process of de-compilation of virtual group trains in large and small interchanges.

(i)Joint hooking: At the time of t_1 moment, the big crossing-up train (m_1 train sets) and the small crossing-up train (m_2 train sets) are joined at the originating station 1, forming the up train of $m_1 + m_2$ set.

(ii)unravelling and return t_2 time, the joint train travelling to the station S_b for unravelling, of which three groups

continue to run to the end of the line to return, the other three groups at the station S_b to return.

(iii)Linking: At the time t_3 , the 3 trains of the returned formation and the 3 trains of formation d arriving at station 2 in the downstream direction are linked to form a downstream 3-train formation.

(iv)Disassemble and turn back: At time t_4 , the downstream 3-unit train arrives at station 1 and then disassembles, with 3-unit trains continuing to the starting point of the line and turning back, and the other 3-unit trains turning back at station 1.

(v) Connecting: At the time t_5 , the three trains returning at Station 1 is connected with the three trains travelling on the Grand Concourse. And so on.

Fig.3 for the virtual group train size of the intersection mode operation process schematic diagram, when the large intersection train running to the small intersection starting station S_a , large intersection train and small intersection train reconnection for the *virtual reconnection train*, by the m_1 grouping of large intersection train and m_2 grouping of small intersection train composition. When the *Virtual Reconnection Train* reaches station S_b , the *Virtual Reconnection Train* will be uncoupled, and the small junction train will turn back at station S_b , the small junction terminal, and continue to run in the small junction section, while the large junction train will continue to run.

B. Analysis of Passenger and Freight Flows

When virtual coupled trains operate on large and small routes, the virtual reconnected train carriages operate independently. The departure frequencies in large and small routes are different, requiring the classification of passenger and freight flows based on passenger travel paths. According to the origin and destination points, passenger (freight) flows can be divided into 12 categories, as shown in Figures 4 and 5: Categories 1-6 represent the upstream direction of passenger (freight) flows, and Categories 7-12 represent the downstream direction.

Taking the upstream direction as an example, Categories 1, 2, 3, and 6 have starting points in the large route section, requiring boarding only on large route trains. Category 4 has origin and destination points in the small route section, allowing boarding on large and small route trains. Category 5 starts in the small route section and ends in the large route section, offering the choice of a direct journey on a large route train or transferring to a large route train after taking a small route train to the station S_b ; downstream passenger (freight) flows exhibit similar characteristics.

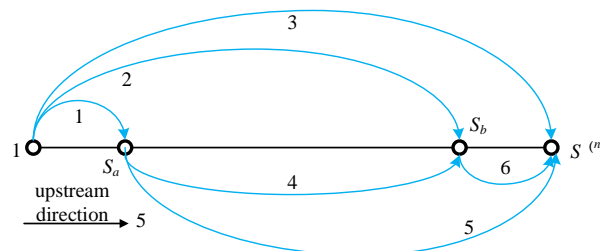


Fig. 4. Passenger flow classification in upstream direction

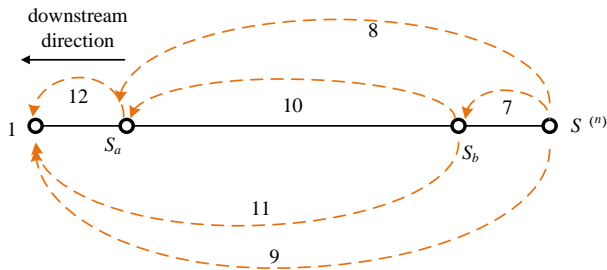


Fig. 5. Passenger flow classification in downstream direction

III. MODEL COSTRUCTION

A. Model Assumption

To construct a rigorous optimization model for the collaborative transportation optimization of passengers and freight, the following basic assumptions are made:

Assumption 1: Passenger and freight demands are known quantities, and the total demand for passengers and freight does not change.

Assumption 2: All carriages have the exact specifications, with identical load capacity and power consumption facilities.

Assumption 3: Passenger and freight carriages operate independently, with passenger carriages not transporting goods throughout the journey and vice versa.

Assumption 4: Large and small route trains operate independently, using a fixed train configuration, without considering the impact of minor route reversals on extensive routes.

B. Objective Function

The symbols and parameters involved in this paper and their related definitions in this paper include:

$S = \{1, 2, \dots, i, j, \dots, S^{(n)}\}$ — The set of stations, $S^{(n)}$ is the total number of stations, and i, j are the station indices.

$S^{(F)} \in S$ — Alternative collection of stations that can handle freight services.

$h = \{h|1, 2\}$ — Intersection type, $h = 1$ denotes Full-length routing, $h = 2$ denotes Short-turn routing.

$K = \{K_1, K_2\}$ — The set of trains.

$K_1 = \{1, 2, \dots, k, \dots, K_1^{(n)}\}$ — The set of Short-turn routing trains, $K_1^{(n)}$ is the total number of trains and k is the index of trains.

$K_2 = \{1, 2, \dots, r, \dots, K_2^{(n)}\}$ — The set of Full-length routing trains, $K_2^{(n)}$ is the total number of trains and r is the index of trains.

g — acceleration of gravity, taken as 9.81 m/s^2 in this paper.

σ — Length of discrete time intervals.

m_h — Number of vehicles in the h routing trains, vehicles.

d_i — Distance between stations i and $i + 1$, $km, i \leq S^n - 1$

ST^i — Stopping time of the train at the station i , min.

ZT_h — h routing Train turnaround time, min.

h_{\max}, h_{\min} — Maximum and minimum safe train departure time, min.

F^P, F^q — Rated capacity of passenger compartment and rated capacity of freight compartment per unit, person/carton

E_p, E_q — Carbon emission factors for rail passenger Transport and carbon emission factors for rail freight Transport.

$C_{k,i}^{(p)}, C_{k,i}^{(q)}$ — Maximum capacity of train k for passengers and maximum capacity for freight.

$p_{i,j}^{(d)}(t), q_{i,j}^{(d)}(t)$ — Passenger and freight flow demand from station i to station j arriving in time slot t .

α, β — Proportion of passengers and freight transported in transport programs.

t_y — Hours of operation of the metro, h.

t_n — Total length of the study period, h.

E_t — Percentage of carbon emissions from train running.

c_{21} — Unit train acquisition cost, yuan.

D_h — Routing length of h routing, km.

Q_s — Carbon emission credits to be purchased by enterprises under the carbon trading policy, kg.

ϕ — Carbon tax charged by the government for each unit of carbon emissions generated by a business.

U_s — Carbon credits for enterprises under the carbon trading policy, kg.

\mathcal{P} — Purchase price per unit of carbon emissions, kg.

θ — Brightness of lamps and air-conditioning intensity in freight trains.

U_t — Corporate carbon allowances, kg.

ϖ — Excess Indicator Variables under Carbon Trading Policies.

and the decision variables for constructing the model in this paper include:

f_h — decision variable, the frequency of train departures on large and small interchanges, pairs/h.

λ — decision variable, ratio of trains running on large and small interchanges.

χ_i — decision variable, minor interchange turnaround indication variable, yes $\chi_i = 1$, otherwise $\chi_i = 0$.

A_k^i — the moment of arrival of a train, indicating the moment when train k arrives at station i .

D_k^i — the moment of departure of the train, indicating the moment when train k leaves station i .

$\alpha_k^i(t)$ — a departure indicator variable, indicating whether train k has left station i at time t , 1 for yes, 0 for no;

m_h — the number of cars in the formation of trains of all sizes of interchanges, vehicles.

$n_k^{(p)}, n_k^{(q)}$ — decision variables, the total number of freight carriages assigned to train k and the total number of freight carriages.

$P_{k,i}^{(p)}, P_{k,i}^{(q)}$ —the passenger and freight capacity of train k when it leaves station i ;

$U_{k,i}^{(p)}, U_{k,i}^{(q)}$ —the number of passengers and freight loaded when train k is at station i ;

$P_{k,i,j}^{(q)}$ —loading of train k to station j when it leaves station i ;

$X_{k,i}^{(p)}, X_{k,i}^{(q)}$ —the number of passengers disembarked and the quantity of goods offloaded when train k arrives at station i ;

$p_i^{(w)}(t)$ —the number of passengers arriving at station i at time t ;

$q_i^{(w)}(t)$ —the number of freights arriving at station i at time t ;

ξ_i —0-1 decision variables, indicating carbon emission policy selection, $i=1,2,3$, representing mandatory carbon emission policy, carbon tax policy, and carbon trading policy, respectively;

PC_{sub} —electricity consumption for train operation during urban railway operation, including electricity consumption for train traction and electricity consumption for ventilation, air-conditioning, lighting and signaling systems, kw/h.

P_f —train traction power, kw.

P_{de} —electrical power of train air-conditioning, lighting and signaling systems, kw.

P_μ —vehicle adhesion mass, tons.

ρ_1, ρ_2, ρ_3 —the empirical coefficients of basic resistance, in this paper, are 2.4, 0.014, 0.001293^[32]

v —train operating speed, km/h.

ρ_{air} —number of luminaires per carriage, group.

s_{ve} —Surface area inside the carriages, m².

Te —Difference in temperature between inside and outside the compartment, °C.

B.1. Passenger Travel Costs

Passenger travel costs include passenger time costs (waiting time, travel time, transfer time) and ticket purchase costs. In Chinese urban rail transit, ticket prices are determined based on the origin and destination of passengers, so ticket prices remain relatively fixed when OD remains constant. With a constant train operating speed, the travel time for a single journey under the same OD will not change, and transfer time is represented by multiplying the waiting time by the transfer penalty coefficient. Therefore, this study mainly considers passenger waiting time.

In the upstream direction, Categories 1, 2, 3, 4, and 6 can board any arriving train to reach their destination station without transferring. The waiting time for passengers can be expressed as the sum of the product of the number of waiting for passengers in each discrete time interval and the length of the discrete time interval.

$$T_{52} = (1 - \mu) \cdot \left(\sum_{i < j} \sum_{t \in T} p_{i,j}^{(w)}(t) \cdot \sigma + \sum_{i < j} \sum_{t \in T} p_{i,j}^{(w)}(D_k^{S_b}) \cdot \sigma \right), i \in [S_a, S_b], j \in [S_b, S^n] \quad (7)$$

$$T_1 + T_2 + T_3 = \sum_{i < j} \sum_{t \in T} p_{i,j}^{(w)}(t) \cdot \sigma, i \in [1, S_a], j \in [1, S_b] \quad (1)$$

$$T_4 = \sum_{i < j} \sum_{t \in T} p_{i,j}^{(w)}(t) \cdot \sigma, i, j \in [S_a, S_b] \quad (2)$$

$$T_6 = \sum_{i < j} \sum_{t \in T} p_{i,j}^{(w)}(t) \cdot \sigma, i, j \in [S_b, S^n] \quad (3)$$

For Category 5 passengers, who start in the small route section and end in the large route section, there are two options: 5a passengers choose the direct journey on a large route train, and 5b passengers choose to take a small route train to the station S_b and transfer to a large route train. The passenger's waiting time is introduced with a preference coefficient $\mu(0 \leq \mu \leq 1)$ representing the probability of choosing the direct journey. The waiting time is then calculated as shown in (4),

$$T_{51} = \mu \cdot \sum_{i < j} \sum_{t \in T} p_{i,j}^{(w)}(t) \cdot \sigma, i \in [S_a, S_b], j \in [S_b, S^n] \quad (4)$$

$$k^i = \begin{cases} M, t = 0 \\ k, D_k^i = t \\ k + 1, D_k^i \leq t \leq D_{k+1}^i \end{cases}, \forall k \in K \quad (5)$$

$$p_{i,j}^{(d)}(D_k^{S_b}) = (1 - \mu) \cdot p_{i,j}^{(d)}(t) \quad (6)$$

For the transfer scheme, passengers depart from train k^i upon its first arrival and alight at station S_b , waiting for the mainline train to transfer. At this point, the origin and destination of this passenger flow are located in the small line section, belonging to the category 5a passenger flow. Subsequently, passengers wait at station S_b and continue their journey, with the origin and destination of this portion of the passenger flow in the mainline section, categorized as 6th class passenger flow. This can be converted into the additional demand $p_{i,j}^{(w)}(D_k^{S_b})$ for station S_b at time $D_k^{S_b}$.

Therefore, the total waiting time for category 5b passenger flow is calculated as shown (7):

In daily life, transfers usually incur additional travel costs for passengers. Hence, a transfer waiting time penalty factor is introduced ν to represent the inconvenience brought to passengers by transfers. The total waiting time for category 5 passenger flow is shown (8).

The downstream passenger flow follows a similar pattern. To convert waiting time into travel costs, this paper employs the non-working time value to measure the value of passenger time. The travel cost for passengers in both large and small line sections is the product of the total waiting time and the value of non-working time per capita in the city, expressed as shown (9).

Where c_1 is the value of non-working time per capita in the city, yuan per minute GDP is the Gross Domestic Product of the city for the current year in thousands of yuan; R is the number of employed people in the city in tens of thousands; and T represents the average working time of the employed population in the city.

$$T_3 = T_{s1} + T_{s2} = T_{s1} = [\mu + \nu(1 - \mu)] \cdot \sum_{i < j} \sum_{t \in T} p_{i,j}^{(w)}(t) \cdot \sigma + (1 - \mu) \cdot \sum_{i < j} \sum_{t \in T} p_{i,j}^{(w)}(D_k^{S_b}) \cdot \sigma, i \in [S_a, S_b], j \in [S_b, S^n] \tag{8}$$

$$F_1 = c_1 \times T \tag{9} \qquad c_1 = 0.3 \times \frac{GDP}{R \times T} \tag{10}$$

$$F_2 = F_{21} + F_{22} \tag{11} \qquad F_{21} = \frac{c_{21} \times N_1}{T_y} \tag{12}$$

$$N_1 = \frac{f_1 \times \left(\sum_{i=1}^{S^{(n)-1}} R^i + \sum_{i=1}^{S^{(n)}} ST^i + 2 \times ZT_1 \right)}{3600} + \frac{f_2 \times \left(\sum_{i=S_a}^{S_b} R^i + \sum_{i=S_a}^{S_b} ST^i + 2 \times ZT_2 \right)}{3600} \tag{13}$$

$$F_{22} = \frac{c_{22} \times \nu \times \left[f_1 \times \left(\sum_{i=1}^{S^{(n)-1}} R^i + \sum_{i=1}^{S^{(n)}} ST^i + 2 \times ZT_1 \right) + \left(f_2 \times \left(\sum_{i=S_a}^{S_b} R^i + \sum_{i=S_a}^{S_b} ST^i + 2 \times ZT_2 \right) \right) \right]}{3600} \tag{14}$$

B.2. Operating Costs of Enterprises

The operating costs of enterprises mainly include the train operation costs related to the kilometers traveled by the train and the train procurement costs allocated to each hour. Specifically, where (12) represents the train procurement cost [33]. The number of vehicles is calculated using (13). The operating cost of the train is the product of the train's per-kilometer operating cost and the kilometers traveled by the train, as given by (14).

B.3. Carbon Emission Costs

The optimizable carbon emissions during subway operation are mainly concentrated in the impacts generated by subway trains' traction, ventilation, air conditioning, lighting, signal systems, etc. Under the conditions of coordinated transportation of passengers and freight, freight transportation can reduce carbon emissions by reducing the use of lighting equipment in freight railway vehicles without affecting transportation and counting operations [18]. This can effectively promote the construction of "green" transportation. The carbon emission *Ce* can be expressed as (15).

$$Ce = PC_{sub} \cdot \alpha \cdot E_p + PC_{sub} \cdot \beta \cdot E_q \tag{15}$$

$$\alpha = \frac{\sum_{k \in K} n_k^{(p)}}{\sum_{k \in K} m_k} \tag{16}$$

$$\beta = \frac{\sum_{k \in K} n_k^{(q)}}{\sum_{k \in K} m_k} \tag{17}$$

$$PC_{sub} = (P_F + P_{de}) \cdot \sum_{k \in K} \sum_{i \in S} (R_k^i + S_k^i) \tag{18}$$

The work done by the train during its operation is calculated by (21) [34]. The electrical power of the train's air conditioning, lighting, and signal systems is calculated by (22).

Under different carbon emission policies, there are differences in carbon emission costs. Under mandatory carbon emission policies, the government requires enterprises to limit their carbon emissions within a certain quota *U_t*.

The cost of carbon emissions within the quota is a fixed value *Ce₁*. Under carbon tax policies, the government imposes a fixed tax rate *φ* on the unit of carbon emissions produced by enterprises. Under carbon trading policies, additional emission allowances must be purchased if carbon emissions exceed the quota. At the same time, enterprises can sell the saved carbon emission allowances externally. This paper introduces 0-1 decision variables to ensure a single carbon emission policy background. Therefore, the carbon emission cost can be expressed as. The operating costs of enterprises mainly include the train operation costs related to the kilometers traveled by the train and the train procurement costs allocated to each hour. Specifically,

$$F_\mu = P_\mu \cdot g \cdot \left(0.24 + \frac{12}{100 + 8\nu} \right) \tag{19}$$

$$\omega_0 = \rho_1 + \rho_2 \cdot \nu + \rho_3 \cdot \nu^2 \tag{20}$$

$$P_F = (F_\mu + \omega_0 \cdot P_\mu \cdot g) \times \sum_{h=1,2} m_h \cdot L_h \cdot \frac{1}{3600} \tag{21}$$

$$P_{de} = \frac{(\sum_{k \in K} n_k^{(p)} + \theta \cdot \sum_{k \in K} n_k^{(q)}) (40 \cdot \rho_{air} + 6 \cdot S_{ve} \cdot Te + 2 \cdot 230)}{3600} \tag{22}$$

$$F_3 = Ce_1 \cdot \xi_1 + Ce \cdot \xi_2 \cdot \phi + Ce \cdot \xi_3 \cdot [(-\vartheta \cdot \varpi) + (1 - \varpi) \cdot \vartheta] \tag{23}$$

C. Model Constraints

C.1 Train travel-related constraints

(24) is the departure interval time constraint for trains of large and small groupings; (25) and (26) are the association constraints between train arrival, departure and stopping times, and interval running hours and minutes; (27) constructs the upper limit constraints on the allocation of freight cars for trains of large and small interchanges; (28) constructs the association constraints on the number of passenger and freight cars in trains; (29) ensures that the trains under the conditions of virtual grouping, taking into account the length of the platforms (29) ensures the feasibility of the maximum number of trains under the virtual formation condition considering the platform length; (30) constructs the constraint on the number of available trains; (31) and (32) construct the constraint on the number of available vehicles and the correlation relationship

between the utilised vehicles and the frequency of operation and the type of formation, and (33) ensures the feasibility of the return of the small interchanges.

$$h_{\min} \leq \frac{60}{f_h} \leq h_{\max}, h=1,2 \quad (24)$$

$$A_k^i = A_k^1 + \sum_{u=1}^{i-1} R_k^u + \sum_{u=1}^{i-1} S_k^u, \forall k \in K, \forall i \in S \quad (25)$$

$$D_k^i = A_k^i + S_k^i, \forall k \in K, \forall i \in S \quad (26)$$

$$0 \leq n_h^{(q)} \leq m_h, h=1,2 \quad (27)$$

$$n_h^{(p)} = m_k - n_h^{(q)} \quad (28)$$

$$m_1 + m_2 \leq m^{\max} \quad (29)$$

$$N_1 \leq N \quad (30)$$

$$\sum_{h=1,2} M_h \leq M \quad (31)$$

$$M_h = \sum_{h=1,2} \frac{60}{f_h} \times m_h \quad (32)$$

$$\sum_{i \in S} \chi_i / 2 = 2 \quad (33)$$

C.2 Passenger flow loading related constraints

(34) constructs the constraints related to the remaining capacity of the train, (35) and (36) construct the loading constraints for the boarding and alighting passenger flow, (37) constructs the constraints related to the number of passengers waiting for the train at the station, and (38) constructs the train departure indicator variable.

$$C_{k,i}^{(p)} = \begin{cases} F^p \cdot n_h^{(p)}, i=1, S^{(n)} \\ C_{k,i-1}^{(p)} - U_{k,i-1}^{(p)} + X_{k,i}^{(p)}, others \end{cases}, \forall k \in K, h=1,2 \quad (34)$$

$$U_{k,i}^{(p)} = \begin{cases} 0, i = S^n \\ \sum_{i < j} \sum_{t \in T} p_{i,j}^{(d)}(t), others \end{cases}, \forall k \in K, \forall i, j \in S \quad (35)$$

$$X_{k,i}^{(p)} = \begin{cases} 0, i=1 \\ \sum_{i < j} \sum_{t \in T} p_{i,j}^{(d)}(t), others \end{cases}, \forall k \in K, \forall i, j \in S \quad (36)$$

$$p_i^{(w)}(t) = \begin{cases} \sum_{i < j} p_{i,j}^{(d)}(t), t=0 \\ p_{i,j}^{(w)}(t-1) + \sum_{i < j} p_{i,j}^{(d)}(t) - \sum_{k \in K} U_{k,i}^{(p)} \cdot \alpha_{k,i}(t), others \end{cases} \quad (37)$$

$$\alpha_k^i(t) \geq \alpha_k^i(t-1) \quad (38)$$

C.3 Freight flow loading related constraints

(39) ensures the fulfillment of all cargo transport requirements, (40) and (41) construct the constraints on the number of freight loaded and cargo unloaded, and further construct the freight on-board constraints (42), and (46) constructs the correlation constraints between the train's freight carrying capacity and the type of formation.

$$\sum_{k \in K} P_{k,i,j}^{(q)} = \sum_{i < j} \sum_{t \in T} q_{i,j}^{(d)}(t), \forall i, j \in S^{(F)} \quad (39)$$

$$U_{k,i}^{(q)} = \begin{cases} 0, i = S^n \\ \sum_{i < j} \sum_{t \in T} q_{i,j}^{(d)}(t), others \end{cases}, \forall k \in K, \forall i, j \in S^{(F)} \quad (40)$$

$$X_{k,i}^{(q)} = \begin{cases} 0, i=1 \\ \sum_{i < j} \sum_{t \in T} q_{i,j}^{(d)}(t), others \end{cases}, \forall k \in K, \forall i, j \in S^{(F)} \quad (41)$$

$$P_{k,i}^{(q)} = \begin{cases} P_{k,i}^{(q)}, i=1 \\ P_{k,i-1}^{(q)} - X_{k,i}^{(q)} + U_{k,i}^{(q)}, others \end{cases}, \forall k \in K, \forall i \in S^{(F)} \quad (42)$$

$$C_{k,i}^{(q)} = \begin{cases} F^q \cdot n_h^{(q)}, i=1, S^{(n)} \\ C_{k,i-1}^{(q)} - U_{k,i-1}^{(q)} + X_{k,i}^{(q)}, others \end{cases}, \forall k \in K, h=1,2 \quad (43)$$

C.4 Carbon emission-related constraints

(44) ensures that only one carbon emission policy can be selected by the model; (45) is the carbon emission limit constraint under the mandatory carbon emission policy, which is a considerable constant; (46) is a set of mutually exclusive constraints constructing the sell quota constraints and the buy quota constraints under the carbon trading policy; and (47) constructs the indicator variable of whether the firms are over-exceeding the quota under the carbon trading policy.

$$\sum_{i=1}^4 \xi_i = 1 \quad (44)$$

$$F_2 \leq U_t \cdot E_t \cdot \frac{t_n}{t_y} \cdot \frac{1}{2} \cdot \xi_1 + (1 - \xi_1) \cdot M \quad (45)$$

$$\begin{cases} (Ce - Q_s) \cdot \xi_3 \cdot \varpi = U_s \cdot \xi_3 \cdot \varpi \\ (Q_s - Ce) \cdot \xi_3 \cdot (1 - \varpi) = U_s \cdot \xi_3 \cdot (1 - \varpi) \end{cases} \quad (46)$$

$$\varpi = \begin{cases} 1, Ce \leq Q_s \\ 0, Ce > Q_s \end{cases} \quad (47)$$

IV. CASE STUDY

A. Case Background

This paper is based on the Wuxi Metro Line 3 (from now on referred to as Line 3) to carry out case analysis and verify the model's validity.

TABLE I
VALUES OF PARAMETERS

Symbols	Values & Units	Symbols	Values & Units
ϕ	35 USD/ton	θ	1min
D_l	28.493km	ST^i	1min
σ	1min	Te	15°C
E_p	0.027 ^[35]	E_q	0.008 ^[35]
$F^{(p)}$	230	h_{\min}	3min
$F^{(q)}$	40 carriages	h_{\max}	10min
s_{ve}	272.08 m ²	v	75km/h
ρ_{air}	10	μ	0.7

B. Result Analysis

Based on the model and algorithm presented in this paper, the carbon tax policy was applied using Matlab 2021 to solve a model with a population size of 200. The Pareto frontier after 200 iterations is depicted in Fig.9, and the optimization results are shown in Table II. Additionally, Fig.10 illustrates the running diagrams of optimization results for both passenger and freight co-transportation schemes within virtual formation train size interchanges. Furthermore, Fig.11 displays the interchanges and formations for Line 3's transport scheme. The findings from Table II indicate that implementing passenger and freight cooperative transport improves average total rates by 6.5%, 5.0%.

And 6.8% under fixed-format operation scheme conditions, fixed-format large- and small-sized intersection operation schemes, as well as virtual-format train operation schemes respectively; thus confirming its effectiveness for composite urban rail transit airport lines. respectively, which verifies the superiority of the virtual-crew train size intersection transport scheme. This paper compares the section fullness rate and average waiting time of passengers at stations of the current transport scheme of Line 3 with the optimized scheme of this paper; as shown in Fig.12, the

optimized scheme can improve the section fullness rate by about 8%-50% in different sections, of which the small junction section is self-explanatory. The average waiting time of passengers at different stations increases by about 0%-1%, of which the passenger and freight co-operation station in the small junction section is more prominent.

C. Discussion and analysis

C.1 Starting and ending station of the Short-turn Routing

The size of the above intersection scheme (optimal scheme), fixed frequency, and other parameters, considered in the ability to return to the station to choose a different site to build minor intersections, to explore the location of the return station to choose the impact on the opening program, the results of the calculations are shown in Table III.

From Table III, it can be seen that, in Scenarios 2 and 3, if the ratio of passenger and freight demand is more excellent than 60%, the proportion of passenger flow in the intersection is higher than the optimal scenario because of the higher proportion of passenger and freight flow in the intersection, so the waiting time of a large number of passengers located in the intersection is reduced, which results in a lower cost of the passengers than the optimal scenario.

TABLE II
OPTIMAL TRAIN PLANS OF PARAMETERS

Modes of Transport Organization	Modes of Routing	Whether to use full and short routing	Full-length Routing			Short-turn Routing			Turnback Station	Modes of Transport Organization No.
			Frequency of train Departures (couple /h)	Coupling Number for Passenger (carriage)	Coupling Number for Freight (carriage)	Frequency of train Departures (couple /h)	Coupling Number for Passenger (carriage)	Coupling Number for Freight (carriage)		
Passenger-only Transportation	Fixed Coupling	-	7	6	-	-	-	-	1~21	1
	Fixed Coupling	√	8	6	-	8	3	-	5~15	2
	Virtual Coupling		7	4	-	7	2	-	5~15	3
Simultaneous passenger and Freight Transportation	Fixed Coupling	-	7	6	2	-	-	-	1~21	4
	Fixed Coupling	√	8	6	1	8	3	1	5~15	5
	Virtual Coupling		7	4	1	7	2	1	5~15	6

TABLE II CONTINUATION
OPTIMAL TRAIN PLANS OF PARAMETERS

Modes of Transport Organization No.	Passenger Travelling Costs (RMB 10,000)	Carbon Emission Cost (RMB 10,000)	Operating Costs (RMB 10,000)	Average Full-load rate(%)
1	6390.1	58866.2	13763.8	20.1
2	6318.7	63071.9	15686.3	16.6
3	6349.9	51016.1	10000.5	59.9
4	6501.6	58100.2	13763.8	46.6
5	6449.7	62100.2	15686.3	39.6
6	6549.9	50055.1	10000.5	66.7

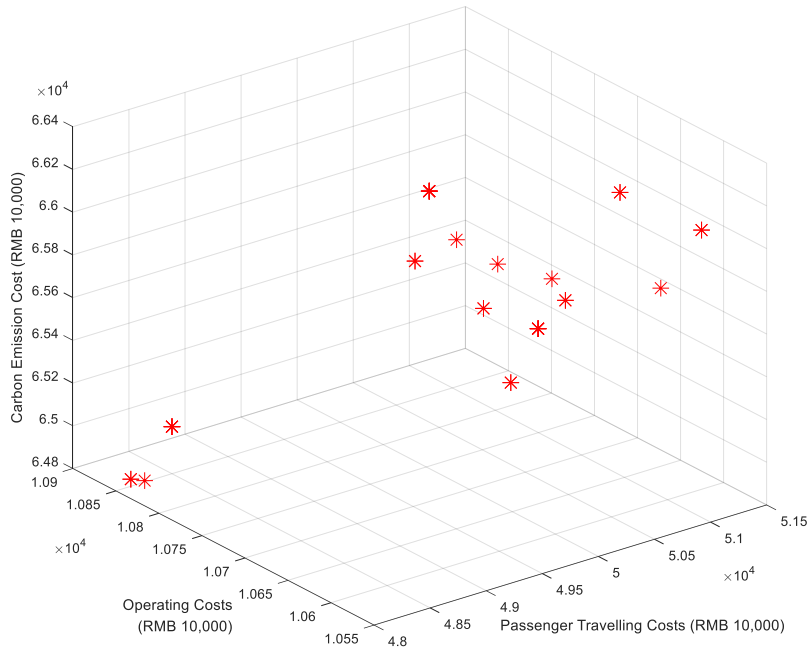


Fig. 9. The Pareto front

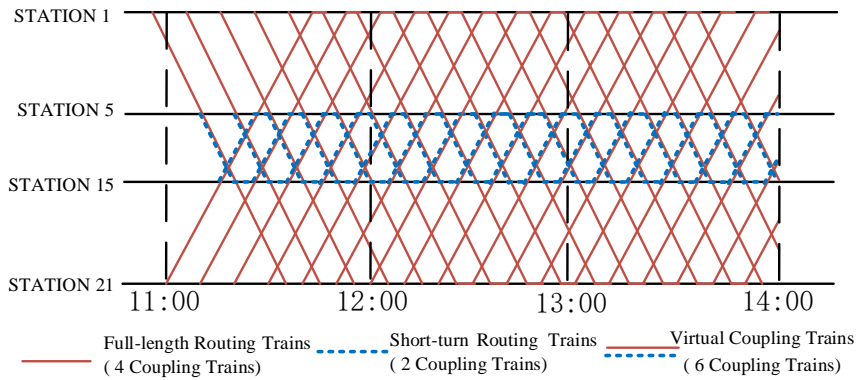


Fig. 10. Train operation diagram of the optimized scheme for Line 3

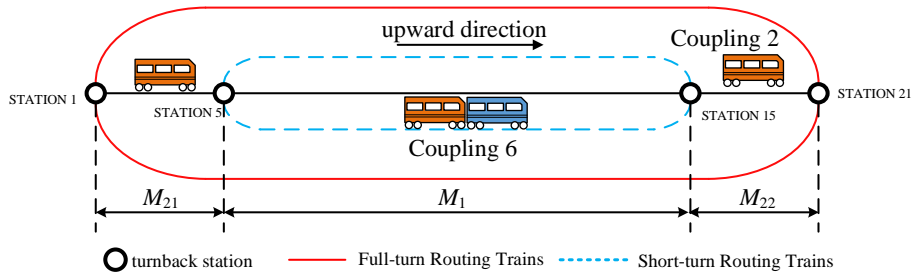


Fig. 11. Scheme of train routings and formations for Line 3

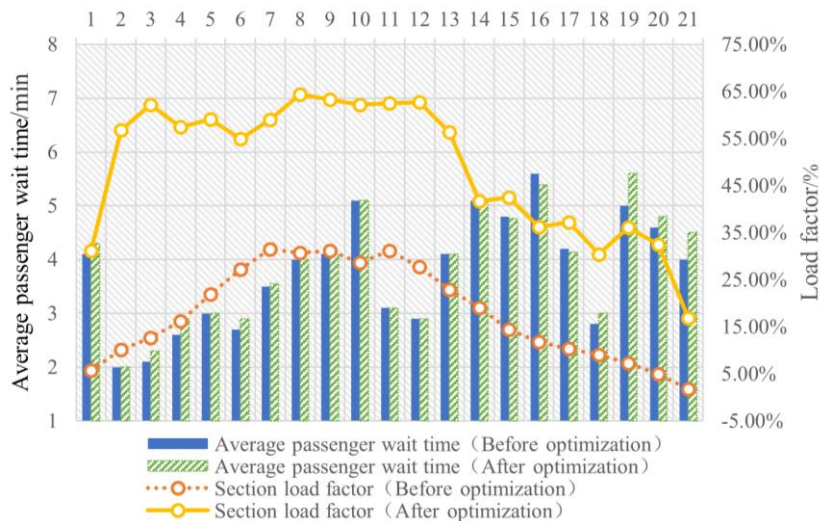


Fig. 12. Section fullness rate and average passenger wait time of Line 3

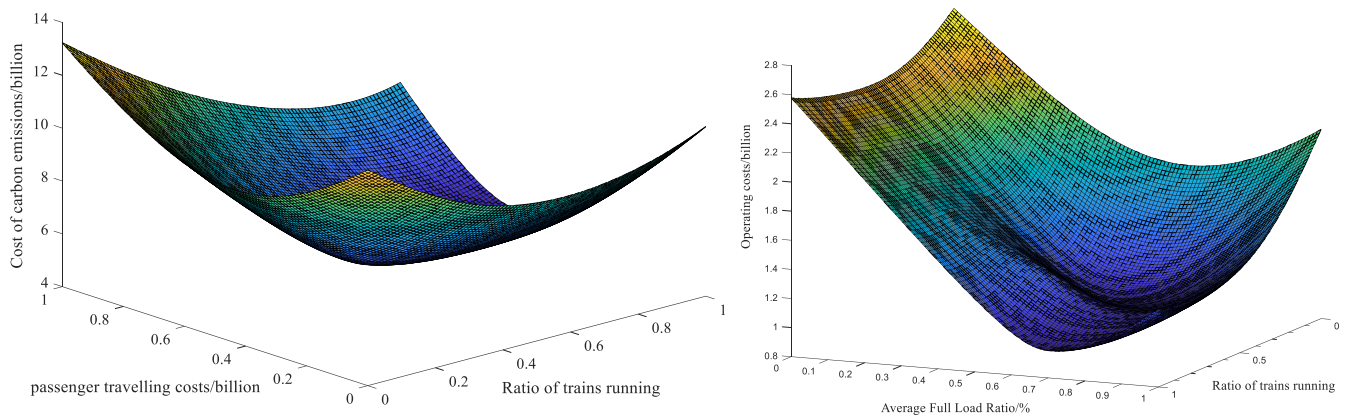


Fig. 13. Parameter perturbation analysis diagram

TABLE III
INFLUENCE OF SHORT-TURN STATION LACATIONS
ON THE OBJECTIVE FUNCTION

No.	Turnback Station	The length of Short-turn routing/km	The passenger percentage of Short-turn routing %	Passenger Travelling Costs (RMB 10,000)	Carbon Emission Cost (RMB 10,000)	Operating Costs (RMB 10,000)	Average Full-load rate/%
1	5~15	13.248	76.1	6549.9	50055.1	10000.5	66.7
2	5~12	11.951	61.1	6672.4	57874.8	12016.9	69.3
3	5~20	19.543	87.6	6731.6	60869.2	16986.4	53.2
4	9~15	7.315	46.6	6592.1	56874.7	11001.3	52.5
5	9~20	17.400	58.1	6631.7	58165.9	18965.9	46.3
6	12~15	4.335	22.3	6988.8	47429.8	9446.6	74.8

Which shows that the proportion of passenger flow in the intersection should be increased in choosing the location of the turnback station. The average section complete rate increases by 2.6% in Scenario 2, which does not include stations 14 and 15, which have the highest passenger flow. Moreover, in Scenario 2, the minor interchanges do not include stations No. 14 and No. 15, which have the highest traffic flow; the average section complete rate increases by 2.6%, and at the same time, the passenger traveling cost increases by 18.7%, which indicates that the minor interchanges should cover the zones with higher traffic flow in the up and down sections in the choice of the return station location.

The combination of the six scenarios shows that the cost of passenger travel decreases as the length of the minor intersection increases. The factors affecting carbon emission and enterprise cost are frequency, intersection distance, and running time. Scheme 6 chooses the smallest intersection distance, but compared with the optimal scheme, the passenger travel cost increases by 6.7%, and the carbon emission cost and enterprise cost are only saved by 5.2% and 5.5%, which shows that when choosing intersections, the operating companies cannot pursue their interests. At the same time, the operation of small and large intersections requires a specific passenger flow base. It is also necessary to have a specific passenger flow base to operate the interchanges of different sizes. There is a significant difference in the distance of interchanges between Scenario 4 and Scenario 3.

However, the carbon emissions and operating costs remain the same linearly with the increase of interchanges, which indicates that the length of small interchanges is shorter than possible.

Accordingly, when designing train interchange schemes, enterprises should not take a single indicator as the deciding factor in formulating interchange schemes. However, they should consider various aspects and reasonably balance the weight of each objective. At the same time, small interchanges during the peak period should cover the intervals with high cross-section passenger flow and cross-section freight flow in the up and down lines to alleviate the pressure of passenger flow and freight flow in these intervals.

C.2 Frequency of train service

Based on the above optimal size of the interchange scheme, other parameters are fixed, and only the ratio of the frequency of trains in the size of the interchange is changed to observe the effect of the ratio on the optimal scheme.

According to Fig.13, when the fixed grouping scheme and interchange scheme, with the increasing frequency of small interchanges, the passenger traveling cost is gradually reduced, but at the same time, the increase of train frequency leads to the growth of carbon emission and enterprise operation cost, and the average total load rate is gradually reduced. Because the value of non-working time per capita is relatively large in the case cities selected in this paper, the curvature of passenger travel costs changes the most with the increase in the frequency of small-transit trains, indicating that for cities with a high value of non-working time per capita, the change in the ratio of the frequency of large and small-transit trains has a more significant impact on the cost of passenger travel. The decision-makers can choose the appropriate ratio of frequency of trains to regulate the cost of passenger travel

according to the actual needs. Between passenger interests, energy saving, and emission reduction, and enterprise cost.

V. CONCLUSION

In order to accelerate the construction of the underground logistics network, from the virtual grouping technology under the large and small interchanges train transport analysis, this paper will discuss the passenger travel costs, enterprise operating costs, and carbon emission costs for the optimization of the tripartite benefits of the target, the small interchanges folding position, car allocation scheme, and train frequency as the primary decision variables, taking into account the balance of passenger and cargo flow, train operation, carbon emission policy constraints to build a virtual grouping based on the urban. The optimal model of the passenger-cargo cooperative transport scheme of airport small and large interchanges of rail transit is constructed. Finally, the optimization scheme of the passenger-cargo cooperative transport of the airport line during the peak period is analyzed by taking the Wuxi Metro Line 3 as an example. The results show that:

(1) The virtual formation technology based on the large and small interchanges operation scheme can reduce the average waiting time of passengers by about 2.01min, the carbon emission cost by 15.7%, and the operating cost of enterprises by 20.2%, and the same time, increase the average total rate by about 50%, which is conducive to the balanced interval between inter-district departures, reduce the travel cost of passengers and the operating cost of enterprises, and achieve the matching of the capacity of different zones, and reduce the carbon emission cost-effectively, which is essential for the study and preparation of urban rail transit train operation diagrams. It is significant for studying and preparing train operation charts for urban rail transit.

(2) Compared with the single-stream passenger transport mode, the passenger and freight cooperative transport mode can (i) increase the average total occupancy rate by about 26.6 percent while increasing the passenger traveling cost by about 0.98 percent, and, at the same time, reduce the carbon emission cost by a small margin; (ii) adopt the traditionally large and small interchanges operation and transport scheme, and increase the average total occupancy rate by about 23 percent with an increase of about 2 percent in passenger traveling cost; and (iii) adopt the virtual formation technology-based operation and transport scheme, and further reduce the carbon emission cost by 1.9 percent while improving the average total occupancy rate by about 5.8 percent. (iii) The adoption of the virtual formation technology-based large and small interchanges operation and transport scheme increases the passenger travel cost by about 0.3 percent while further reducing the carbon emission cost by 1.9 percent and, at the same time, improves the average total occupancy rate by about 5.8 percent.

(3) Under the virtual grouping technology, when designing the large and small junction running scheme, the primary operating companies set up the large and small junction scheme and set up the traditional large and small junction scheme with basically the same principle, the small junction should cover the intervals with high passenger flow in the up and down intersection, and at the same time, it

increases the proportion of small junction passengers to a certain extent, but it is not the longer the distance between the intervals of the small junction, the better the operation effect, and it should be selected according to the actual demand for the foldback Station location; changes in frequency of operation have a more significant impact on passenger travelling costs, decision makers can control the frequency of train operation by adjusting the time value of urban per capita non-working time, and increase the distance of the intersection of small interchanges to reduce the cost of passenger travel.

(4) The model constructed in this paper is a more general multi-objective hybrid planning model under different carbon policies, including mandatory carbon emission policy, carbon tax policy, and carbon trading policy, and it can be adapted to the changes of carbon policies under different development stages by changing some of the parameter settings. The current carbon policy adopted by the government has less influence on the urban rail passenger and freight cooperation scheme, and the model can still have better optimization performance in the future when the government formulates a reasonable carbon policy according to the differences of each industry.

REFERENCES

- [1] MURAKAMI J, MATSUI Y, KATO H, "Airport rail links and economic productivity: Evidence from 82 cities with the world's 100 busiest airports," *Transport Policy*, vol.52, pp. 89-99, 2016.
- [2] G.J. Yang, J.R. Zhang, Z. Fang, "A Review of Research on Evaluation Methods for Green Urban Railway Transport," *Green Building*, no.10(06):pp. 9-12+16, 2018
- [3] SAVELSBERGH M, VAN W T, "50th anniversary invited article-city logistics: challenges and opportunities," *Journal of Transportation Science*, vol. 50, no. 2, pp. 579-590, 2016.
- [4] MOTRAGHI A, and MARINOV M V, "Analysis of urban freight by rail using event-based simulation," *Journal of Simulation Modelling Practice and Theory*, vol. 25, no. 3, pp. 73-89, 2012.
- [5] Y.Y. Yao, Y.Z. Zhang, "Study the express freight transport scheme of high-speed rail in piggyback passenger car mode," *Journal of Railway Science and Engineering*, vol. 17, no 1, pp. 31-38, 2020,
- [6] Y. Z. Chao, R.H. Gao, H.M, Niu. "Optimization of train plan on highspeed railway immediate delivery based on candidate train set," *Journal of Railway Science and Engineering*, vol.19, no.12: pp.3505-3514,2022.
- [7] BRICE D, MARINOV M, RUGER B, "A newly designed baggage transfer system was implemented using event-based simulations," *Urban Rail Transit*, 2015, vol. 1, no. 4, pp. 194-214.
- [8] OZTURK O, and PATRICK J, "An optimization model for freight transport using urban rail transit," *European Journal of Operational Research*, vol. 267, no. 3, pp. 1110-1121, 2018.
- [9] BEHIRI W, BELMOKHTAR B S, and CHU C, "Urban freight transport using passenger rail network: Scientific issues and quantitative analysis," *Journal of Transportation Research Part E: Logistics and Transportation Review*, vol. 115, no. 3, pp. 227-245, 2018.
- [10] Z. Li, SHALABY A, and ROORDA M J, "Urban rail service design for collaborative passenger and freight transport," *Journal of Transportation Research Part E: Logistics and Transportation Review*, vol. 147, no. 4, pp. 102205, 2021.
- [11] Z. Di, L. Yang, and J. Shi, "Joint optimization of carriage arrangement and flow control in a metro-based underground logistics system," *Journal of Transportation Research Part B: Methodological*, vol. 159, no. 2, pp. 1-23, 2022.
- [12] J.G. Qi, H.S. Zhou, and L.X. Yang, "Optimization methods of combined passenger and freight transportation based on flexible train composition mode," *Journal of Transportation Systems Engineering and Information Technology*, vol. 22, no. 2, pp. 197-205, 2022.
- [13] CACCHIANI V, CAPRARA A, and TOTH P, "Scheduling extra freight trains on railway networks," *Journal of Transportation Research Part B*, vol. 44, no. 2, pp. 215-231, 2010.
- [14] Z.Z. Li, Y. Bai, and Y. Chen, "Integrated optimization of train service planning and shipment allocation for airport expresses under mixed

- passenger and freight transportation,” *Journal of Transportation Systems Engineering and Information Technology*, vol. 22, no. 5, pp. 155-163, 2022.
- [15] RICHARD P L, “Carbon footprint report,” *London: Transport for London*, 2019.
- [16] J.Y. Long, “Evaluation model and optimization method of urban passenger transport system based on carbon emission target,” *Wuhan: Huazhong University of Science & Technology*, 2012.
- [17] Y.Z. Dai, S.G. Zhan, “Analysis of full-length and short-turn routing of urban rail transit considering carbon emission,” *Journal of Railway Science and Engineering*, vol. 19, no. 12, pp. 3546-3556, 2022
- [18] H.C. Pan, J.B. Lu, H. Hu, Z.G. Liu, and Y. Sha, “Collaborative optimization of urban rail timetable and flow control under mixed passenger and freight transportation,” *Journal of Transportation Systems Engineering and Information Technology*, vol. 23, no. 2, pp. 187-196, 2023.
- [19] H. Wang, “Optimization Study of Urban Rail Transit Large and Small Interchange Operation Schemes,” *Beijing Jiaotong University*, 2020.
- [20] G.J. Wei, “Study on the Method of Setting Long and Short Crossings for Trains of Urban Rail Transit Lines,” *Beijing Jiaotong University*, 2013.
- [21] L. Deng, Q. Zeng, W. Gao, “Optimization of train plan for urban rail transit in the multi-routing mode,” *Journal of modern transportation (English edition)*, 2011.
- [22] D.F. Liao, “Study on the Design of Urban Railway Large and Small Interchange Running Schemes,” *Chang’an University*, 2019.
- [23] STANDER T, DREWES J, BRAUN I, “Operational and Safety Concepts for Railway Operation with Virtual Train-sets,” *FAC Proceedings Volumes*, vol. 39, no. 12, pp. 261-266, 2006
- [24] Y. Zhang, S.R. Zhang, “Typical Train Virtual Coupling Scenario Modeling and Analysis of Train Control System Based on Vehicle-Vehicle Communication,” *2020 IEEE 6th International Conference on Control Science and Systems Engineering (ICCSSE)*. Beijing, China. pp.143-148, 2020.
- [25] H. Duan, Y. Yang, Y. Duan, J. Zhang. “Research on Virtual Coupling Train Operations Based on Moving-Block and Vehicle-to-Vehicle Communication,” *Journal of Physics Conference Series*, vol. 1631, no. 012004, 2020,
- [26] QUAGLIETTA E, WANG M, and GOVERDE R, “A multistate train-following model for the analysis of virtual coupling railway operations,” *Journal of Rail Transport Planning & Management*, vol. 15, no. 6, pp. 100-195, 2022.
- [27] FLAMMINI F, MARRONE S, NARDONE R, et al.” Towards railway virtual coupling,” *2018 IEEE International Conference on Electrical Systems for Aircraft, Railway, Ship Propulsion and Road Vehicles & International Transportation Electrification Conference (ESARS-ITEC)*. IEEE pp.1-6, 2018.
- [28] Q. Zhang, J.W. Bai, B.M. Han et al. “Fast and slow vehicle real-time marshaling operation organization method adopting virtual marshaling technology: CN113120038B [P] ,” 2022-02-15.
- [29] LEE B, CHAE S, and CHOI H Y, “Skip and stop scheduling based on virtually coupled trains,” *Journal of the Korean Society for Railway*, vol. 23, no. 4, pp. 80-88, 2020.
- [30] GALLO F, FEBBRARO A, and GIGLIO D, “A mathematical programming model for the management of carriages in virtually coupled trains,” *2020 IEEE 23rd International Conference on Intelligent Transportation Systems*. Rhodes, 2020.
- [31] GALLO F, FEBBRARO A, and GIGLIO D, “Planning and optimization of passenger railway services with virtually coupled trains,” *2021 7th International Conference on Models and Technologies for Intelligent Transportation Systems*. Heraklion, 2021.
- [32] J.J. Ning. Research on model and algorithm of energy saving operation for urban rail transit[D]. Beijing: Beijing Jiaotong University, 2017.
- [33] W.Y. Yu, Z.G. Zhu. “The selection method of urban rail transit routing scheme,” *China Transportation Review*, vol. 42, no 9, pp. 54–59, 2020.
- [34] B.H. Mao. Train performance calculation and design [M]. Beijing: China Communications Press, 2008.
- [35] X.Y. Wu, B.H. Mao, Q. Zhou Qi et al. “Comparative of carbon emission factor levels in different modes of transportation industry,” *Journal of East China Jiaotong University*, vol.39, no.4, pp.41-47, 2022.

Zunzun Hou was born in Henan, China, in 1998. She obtained her Bachelor degree in Traffic and Transportation from Lanzhou Jiaotong University, Lanzhou, China, in the year 2021. She is currently pursuing her master degree for Traffic and Transportation (the Transportation Engineering) in Lanzhou Jiaotong University. Her research interests include Optimization of Passenger and Freight Collaborative Transportation and Virtual Coupling.